Published OnlineFirst November 30, 2016; DOI: 10.1158/1078-0432.CCR-16-1025

Biology of Human Tumors

Clinical Cancer Research

Combining Anti-Mir-155 with Chemotherapy for the Treatment of Lung Cancers

Katrien Van Roosbroeck[1], Francesca Fanini[2], Tetsuro Setoyama[1], Cristina Ivan[3,4], Cristian Rodriguez-Aguayo[1,3], Enrique Fuentes-Mattei[1], Lianchun Xiao[5], Ivan Vannini[2], Roxana S. Redis[1], Lucilla D'Abundo[1,6], Xinna Zhang[3,4], Milena S. Nicoloso[7], Simona Rossi[1], Vianey Gonzalez-Villasana[1,3,8], Rajesha Rupaimoole[4], Manuela Ferracin[9], Fortunato Morabito[10], Antonino Neri[11], Peter P. Ruvolo[12], Vivian R. Ruvolo[12], Chad V. Pecot[13], Dino Amadori[2], Lynne Abruzzo[14], Steliana Calin[15], Xuemei Wang[5], M. James You[15], Alessandra Ferrajoli[12], Robert Orlowski[16], William Plunkett[1], Tara M. Lichtenberg[17], Ramana V. Davuluri[18], Ioana Berindan-Neagoe[19,20], Massimo Negrini[6], Ignacio I. Wistuba[13,21], Hagop M. Kantarjian[12], Anil K. Sood[3,4], Gabriel Lopez-Berestein[1,3], Michael J. Keating[12], Muller Fabbri[22], and George A. Calin[1,3,12]

Abstract

Purpose: The oncogenic miR-155 is upregulated in many human cancers, and its expression is increased in more aggressive and therapy-resistant tumors, but the molecular mechanisms underlying miR-155-induced therapy resistance are not fully understood. The main objectives of this study were to determine the role of miR-155 in resistance to chemotherapy and to evaluate anti-miR-155 treatment to chemosensitize tumors.

Experimental Design: We performed *in vitro* studies on cell lines to investigate the role of miR-155 in therapy resistance. To assess the effects of miR-155 inhibition on chemoresistance, we used an *in vivo* orthotopic lung cancer model of athymic nude mice, which we treated with anti-miR-155 alone or in combination with chemotherapy. To analyze the association of miR-155 expression and the combination of miR-155 and *TP53* expression with cancer survival, we studied 956 patients with lung cancer, chronic lymphocytic leukemia, and acute lymphoblastic leukemia.

Results: We demonstrate that miR-155 induces resistance to multiple chemotherapeutic agents *in vitro*, and that downregulation of miR-155 successfully resensitizes tumors to chemotherapy *in vivo*. We show that anti-miR-155-DOPC can be considered nontoxic *in vivo*. We further demonstrate that miR-155 and *TP53* are linked in a negative feedback mechanism and that a combination of high expression of miR-155 and low expression of *TP53* is significantly associated with shorter survival in lung cancer.

Conclusions: Our findings support the existence of an miR-155/TP53 feedback loop, which is involved in resistance to chemotherapy and which can be specifically targeted to overcome drug resistance, an important cause of cancer-related death. *Clin Cancer Res; 23(11); 2891–904. ©2016 AACR.*

[1]Department of Experimental Therapeutics, The University of Texas MD Anderson Cancer Center, Houston, Texas. [2]Istituto Scientifico Romagnolo per lo Studio e la Cura dei Tumori (IRST) S.r.l. IRCCS, Unit of Gene Therapy, Meldola, Italy. [3]Center for RNA Interference and Non-Coding RNAs, The University of Texas MD Anderson Cancer Center, Houston, Texas. [4]Department of Gynecologic Oncology, The University of Texas MD Anderson Cancer Center, Houston, Texas. [5]Department of Biostatistics, The University of Texas MD Anderson Cancer Center, Houston, Texas. [6]Department of Morphology, Surgery and Experimental Medicine, University of Ferrara, Ferrara, Italy. [7]Division of Experimental Oncology 2, CRO, National Cancer Institute, Aviano, Italy. [8]Departamento de Biologia Celular y Genetica, Universidad Autonoma de Nuevo Leon, 66450 San Nicolas de los Garza, Nuevo Leon, Mexico. [9]Department of Experimental, Diagnostic and Specialty Medicine–DIMES, University of Bologna, Bologna, Italy. [10]Department of Onco-Hematology, A.O. of Cosenza, Cosenza, Italy. [11]Department of Clinical Sciences and Community Health, University of Milano and Hematology, Ospedale Policlinico, Milano, Italy. [12]Department of Leukemia, The University of Texas MD Anderson Cancer Center, Houston, Texas. [13]Department of Thoracic/Head and Neck Medical Oncology, The University of Texas MD Anderson Cancer Center, Houston, Texas. [14]Department of Pathology, The Ohio State University, Columbus, Ohio. [15]Department of Hematopathology, The University of Texas MD Anderson Cancer Center, Houston, Texas. [16]Department of Lymphoma/Myeloma, The University of Texas MD Anderson Cancer Center, Houston, Texas. [17]The Research Institute, Nationwide Children's Hospital, Columbus, Ohio. [18]Department of Preventive Medicine, Division of Health and Biomedical Informatics, Northwestern University, Feinberg School of Medicine, Chicago, Illinois. [19]Department of Functional Genomics, The Oncology Institute, Cluj-Napoca, Romania. [20]Research Center for Functional Genomics, Biomedicine and Translational Medicine, University of Medicine and Pharmacy Iuliu Hatieganu, Cluj-Napoca, Romania. [21]Department of Translational Molecular Pathology, The University of Texas MD Anderson Cancer Center, Houston, Texas. [22]Children's Center for Cancer and Blood Disease, Departments of Pediatrics and Molecular Microbiology & Immunology, Norris Comprehensive Cancer Center, Keck School of Medicine, University of Southern California, Saban Research Institute, Children's Hospital Los Angeles, Los Angeles, California.

Note: Supplementary data for this article are available at Clinical Cancer Research Online (http://clincancerres.aacrjournals.org/).

K. Van Roosbroeck, F. Fanini, and T. Setoyama contributed equally to this article.

Corresponding Authors: George A. Calin, The University of Texas MD Anderson Cancer Center, So Campus Research Building 3 (3SCR4.3424), 1881 East Road, Unit 1950, Houston, TX 77054. Phone: 713-792-5461; Fax: 713-745-4528; E-mail: gcalin@mdanderson.org; and Muller Fabbri, Departments of Pediatrics and Molecular Microbiology and Immunology, Children's Hospital Los Angeles, University of Southern California, 4650 Sunset Boulevard, Mailstop # 57, Los Angeles, CA 90027. Phone: 323-361-8920; Fax: 323-361-4902; E-mail: mfabbri@chla.usc.edu

doi: 10.1158/1078-0432.CCR-16-1025

Published OnlineFirst November 30, 2016; DOI: 10.1158/1078-0432.CCR-16-1025

Translational Relevance

Resistance to therapy is an important issue in the treatment of cancer, responsible for many cancer-related deaths. Despite decades of research into overcoming this resistance, only modest advances have been made, and the resistance mechanisms remain poorly understood. This is the first report of a miR-155/TP53-negative feedback mechanism in which there is a direct targeting of *TP53* by miR-155, and which is involved in the resistance to multiple chemotherapeutic drugs used in the treatment of lung cancer and leukemias. The finding that treatment with anti-miR-155 can reverse chemoresistance *in vivo* and that anti-miR-155-DOPC is not toxic *in vivo* supports a potential clinical use of anti-miR-155 therapy in human clinical trials of various cancer types as an addition to current chemotherapy regimens in order to overcome cancer-enacted resistance mechanisms.

Introduction

Resistance to therapy is the leading cause of failure to respond to chemotherapeutic drugs that leads to the high mortality in cancer (1, 2). Despite decades of research, only modest advances have been made in developing strategies to overcome resistance (3). The addition of non-coding RNAs (ncRNAs) to the ever-expanding set of genes deregulated in cancer (4, 5) offers the opportunity to deeper understand these mechanisms and the hope to eradicate chemoresistance. Non–small cell lung cancer (NSCLC) and chronic lymphocytic leukemia (CLL) are the most frequent adult solid and hematological malignancies in the Western world, respectively (2), and resistance to therapy is a very significant medical issue in these patients. Virtually all patients with NSCLC will eventually develop resistance to the chemotherapeutic agents they are exposed to (6), and all patients with CLL requiring treatment, including the standard-of-care chemotherapy-based fludarabine, cyclophosphamide, and rituximab (FCR) treatment, are expected to relapse (7). The poorest-prognosis CLL subgroup is characterized by deletions of chromosome 17p (del17p), the genomic locus of *TP53*, having an overall survival of less than 2 years (8, 9). The tumor suppressor gene *TP53* is frequently deleted or mutated in human cancers and is involved in the development of drug resistance by cancer cells (10).

MicroRNAs (miRNAs) are small ncRNAs that regulate the expression of protein coding genes (11). MiR-155 is a well-known oncogenic miRNA, which is upregulated in a wide variety of human cancers (12, 13), especially in more aggressive and therapy-resistant tumors (14, 15). For example, we identified a signature of deregulated miRNAs in patients with CLL and 17p deletion, versus patients with normal genotype, having good prognosis (16). In the 17p deletion group, miR-155 was the most upregulated miRNA (16). Moreover, we and others have demonstrated that miR-155 has prognostic significance in multiple types of tumors, including leukemia (17, 18) and lung cancer (19, 20).

Overexpression of miR-155 has been associated with drug resistance in several human cancers, including breast cancer, B-cell lymphoma, and colon cancer (14, 21, 22), but the molecular mechanisms through which miR-155 increases cancer cell resistance to treatment are not fully understood. Therefore, the main objectives of this study were to determine the molecular mechanism through which miR-155 induces resistance to chemotherapy and to evaluate anti-miR-155 treatment to chemosensitize tumors. We demonstrate that overexpression of miR-155 induces resistance to chemotherapy, which can be reversed upon miR-155 inhibition. We show that anti-miR-155-DOPC does not induce adverse events and can be considered non-toxic *in vivo*. We further identify a miR-155/TP53-negative regulatory feedback loop that affects the development of cancer drug resistance. The inverse expression correlation between miR-155 and *TP53* transcripts is additionally supported by survival data from four lung cancer cohorts, in which we show that high expression of miR-155 and low expression of *TP53* are associated with shorter survival, further confirming the involvement of miR-155 in TP53-mediated resistance mechanisms.

Materials and Methods

Patient samples

The origin of all patient datasets is presented in Table 1. The total number of patients included in the survival analyses was 956. Both analyzed CLL subgroups were previously described: CLL-NEJM (23) and CLL-Clin Cancer Res (24). Clinical characteristics of both CLL cohorts can be found in Supplemental Tables.

Twenty-four NSCLC samples were collected at the Istituto Scientifico Romagnolo per lo Studio e la Cura dei Tumori (IRST) IRCCS, Italy (NSCLC-Italy), 58 lung adenocarcinoma samples were collected at The University of Texas MD Anderson Cancer Center (lung adenocarcinoma-MDACC), and 52 ALL samples were collected at MDACC (ALL-MDACC). Clinical characteristics of both lung cancer datasets and the ALL dataset can be found in Supplementary Tables S2 and S3, respectively. All patients provided written informed consent prior to inclusion in the study, and collection of the samples was approved by the institutional review board at each institution (IRST Srl IRCCS, and MDACC). All the work described has been carried out in accordance with the Declaration of Helsinki. In addition, the TCGA datasets for lung adenocarcinoma ($n = 343$) and lung squamous cell carcinoma ($n = 192$) were downloaded from the data portal at https://gdc.cancer.gov/ (currently https://gdc.cancer.gov), and survival analysis was performed (Table 1).

Cell culture, transfection, and treatment

Cell lines. Lung cancer cell lines A549, H460, H2009, and H1299 and leukemia cell lines REH and JM1 were purchased from the American Type Culture Collection (ATCC) and cultured following the recommendations in the Product Information Sheet (ATCC). REH cells with TP53 knockdown (REH shp53) were generated by retroviral transduction with the gene-specific shRNA transfer vector pMKO.1 puro p53 shRNA 2 (plasmid 10672, Addgene), as previously described (25). REH cells transfected with the empty vector pMKO.1 puro GFP shRNA (REH wt) were used as negative controls. Cell lines were authenticated via STR DNA fingerprinting and tested for mycoplasma contamination with the MycoAlert Mycoplasma Detection Kit (Lonza) at the time they were cultured for the experiments performed in frame of this research.

miRNA mimics/inhibitor transfection. Transfections were performed with 100 nmol/L of the precursor molecules (hsa-miR-155-5p pre-miRNA precursor or pre-miRNA precursor negative

Published OnlineFirst November 30, 2016; DOI: 10.1158/1078-0432.CCR-16-1025

Table 1. The analyzed patient datasets for survival analysis

Dataset	Reference	Total No. pts	*TP53* survival analysis				miR-155 survival analysis				Combined miR-155 and *TP53* survival analysis			
			No. pts *TP53* high[b]	No. pts *TP53* low	Poor prognosis	*P*	No. pts miR-155 high	No. pts miR-155 low	Poor prognosis	*P*	No. pts miR-155 high/*TP53* low	No. pts miR-155 low/*TP53* high	Poor prognosis	*P*
CLL–NEJM	(23)	94	NA	NA	NA	NA	39	55	high miR-155	**0.0337**	NA	NA	NA	NA
CLL–Clin Cancer Res	(24)	212	NA	NA	NA	NA	105	107	high miR-155	**0.005**	NA	NA	NA	NA
ALL–MDACC	MDACC	52	NA	NA	NA	NA	14	38	high miR-155	**0.0052**	NA	NA	NA	NA
NSCLC–Italy	IRST	24	11	13	/	0.119	9	15	/	0.064	4	13	high miR-155; low *TP53*	**0.0161**
Lung adenocarcinoma–MDACC	MDACC	58	22	36	/	0.06	34	24	/	0.22	26	14	high miR-155; low *TP53*	**0.0356**
Lung adenocarcinoma–TCGA[a]	TCGA	343	216	127	*TP53* low	**0.019**	236	107	/	0.19	90	70	high miR-155; low *TP53*	**0.0177**
Lung squamous cell carcinoma–TCGA	TCGA	192	119	73	/	0.086	136	56	/	0.25	46	29	high miR-155; low *TP53*	**0.0243**
Total		956	368	249			555	401			166	126		

Abbreviations: NEJM, The New England Journal of Medicine; MDACC, The University of Texas MD Anderson Cancer Center; pts, patients.

[a]The TCGA data were downloaded from the data portal at https://gdc.cancer.gov/ (currently https://gdc.cancer.gov).

[b]High and low expression of mir-155 and *TP53* was determined with the log-rank test as indicated in the statistical analysis section of the Materials and Methods.

control #1), 200 nmol/L of the miRVana inhibitors (miRVana hsa-miR-155 inhibitor and miRVana inhibitor negative control #1), and Lipofectamine 2000 reagent or Lipofectamine RNAiMAX reagent, respectively (Life Technologies), according to the manufacturer's instructions. MiRNA transfection efficiencies were evaluated by qRT-PCR.

miR-155 lentivirus infection. pMIRNA1—miR-155 and pMIRNA1—Empty Vectors were obtained from System Biosciences, and viral particles were produced according to the manufacturer's instructions. A549, REH wt, REH shp53 and JM1 cells were infected with the miR-155 lentivirus with an efficiency of approximately 50% as determined by GFP measurement by flow cytometry. Empty lentivirus (LVEV, lentivirus empty vector) was used as a negative control for the experiments.

Drug treatment. Cisplatin (CDDP) was obtained from the oncology pharmacy of MDACC and S.r.l. IRCCS as an aqueous solution at a concentration of 1 mg/mL corresponding to 3.3 mmol/L. Exposures ranged from 0.01 to 10 μmol/L. Doxorubicin (hydrochloride) was purchased as a powder from Sigma-Aldrich and resuspended in dimethyl sulfoxide (DMSO) (Sigma-Aldrich) to a stock concentration of 1.78 mmol/L. Exposures ranged from 0.01 to 0.5 μmol/L.

RNA extraction and quantitative real-time PCR

RNA was isolated with TRIzol (Life Technologies), or with mirVana miRNA Isolation Kit (Ambion, Life Technologies), according to the manufacturer's instructions. MiR-155 expression was analyzed with TaqMan miRNA Assays (Life Technologies). cDNA was synthesized using gene-specific stem-loop reverse transcription primer and the TaqMan microRNA reverse-transcription kit (Life Technologies). Real-time qRT-PCR was carried out in an Applied Biosystems 7500 Real-Time PCR System (Applied Biosystems, Life Technologies) or on a Bio-Rad CFX384 Real-Time PCR Detection System (Bio-Rad Laboratories). Experiments were performed in triplicate and normalized to RNU44, U6, or RNU6B. Relative expression levels were calculated with the comparative Ct method (ΔΔCt).

Protein extraction and Western blotting

Protein extraction and Western blotting were performed as previously described (26, 27). The following primary antibodies were used: anti-Vinculin clone FB11 mouse monoclonal antibody (Biohit, Sartorius), anti-Human/Mouse/Rat p53 goat polyclonal antibody (R&D Systems), anti-$p21^{WAF1}$ Ab-3 (Clone DCS-60.2) mouse monoclonal antibody (Lab Vision, Thermo Fisher Scientific), anti-p21 Waf1/Cip1 (DCS60) mouse monoclonal antibody (Cell Signaling Technology) and anti-TP53DINP1 rabbit polyclonal antibody (OriGene). Western blots were quantified with Photoshop CS6 (Adobe).

Chromatin immunoprecipitation

Chromatin immunoprecipitation (ChIP) was performed with the EZ-ChIP Chromatin Immunoprecipitation kit (EMD Millipore) and the rabbit polyclonal antibody p53 (FL-393) (Santa Cruz Biotechnology) according to the manufacturer's instructions. The TP53 binding sites in miR-155 (TP53 BS1/2 and TP53 BS3) were amplified with RedTaq DNA polymerase (Sigma-Aldrich) using the primers below and analyzed on a 2% agarose gel.

Published OnlineFirst November 30, 2016; DOI: 10.1158/1078-0432.CCR-16-1025

TP53 BS1/2 ChIP FW 5′-GATCAAAGGATTCTCACCTGGG-3′
TP53 BS1/2 ChIP RV 5′-ATCTGAACTACCTGGTCAGCCTGT-3′
TP53 BS3 ChIP FW 5′-AGCAGGGTAAATAACATCTGACAGC-3′
TP53 BS3 ChIP RV 5′-CATATGGAGGAAGAAACAGGCTTAG-3′

Luciferase assay and mutagenesis

Identification of putative TP53 binding sites within a 10-kb genomic region surrounding miR-155 was performed by a TP53-binding site prediction program, which we developed earlier (28, 29). The identified TP53 binding site BS3 downstream of the miR-155 gene was cloned in the pGL4.23 (luc2/minP) vector (Promega) with the following primers (underlined are the added restriction sites):

TP53 BS3 FW 5′-GCGGTACCGGGAAACTGAAAGGCTATGAA-3′
TP53 BS3 RV 5′-GCGCTAGCCCCCATATGGAGGAAGAAAC-3′

A549 cells were seeded at 50,000 cells/well in 24-well plates and cotransfected with the pGL4.23 vector containing the predicted TP53 binding site, the pCMV6-XL5-TP53 expressing vector (OriGene) and the pGL4.74 (hRluc/TK) vector containing renilla luciferase. Twenty-four hours after transfection, the samples were analyzed with the Dual-Luciferase Reporter Assay System (Promega) in a Glomax 96 Microplate Luminometer (Promega) as described in the manufacturer's manual. Mutagenesis of the TP53 recognition sequence BS3 was performed with the QuickChange XL Site-Direct Mutagenesis Kit (Stratagene, Agilent Technologies), which deleted a portion of the TP53 consensus sequence, according to the manufacturer's instructions, and with the following primers:

TP53 BS3-DEL FW 5′-CATATTTGAAATGTCTAGGTTCAAGTTCAATAGCTTAGCC-3′
TP53 BS3-DEL RV 5′-GGCTAAGCTATTGAACTTGAACCTAGACATTTCAAATATG-3′

Identification of putative miR-155 binding sites in *TP53* was performed with RNAhybrid (v2.2; ref. 30). The identified miR-155 binding sites in *TP53* [in coding sequence, BS-CDS; in 3′ untranslated region (UTR), BS-UTR] were cloned in a pGL3 Control vector (Promega) with the following primers (underlined are the added restriction sites):

miR-155 BS-CDS FW 5′-GGACTAGTCATGAGCGCTGCTCAGATAG-3′
miR-155 BS-CDS RV 5′-TCCCCGCGGGCCCATGCAGGAACTGTTA-3′
miR-155 BS-UTR FW 5′-GGACTAGTAAGGAAATCTCACCCCATCC-3′
miR-155 BS-UTR RV 5′-TCCCCGCGGAAGGCTGCAGTAAGCCAAGA-3′

H1299 and H460 were seeded and transfected as mentioned above. Luciferase assays and mutagenesis of the identified binding sites were carried out as mentioned above. The following primers, which deleted the miR-155 binding site, were used:

miR-155 BS-CDS-DEL FW
5′-GGTCTGGCCCCTCCTCAGCATTTGCGTGTGGAGTATTTGG-3′
miR-155 BS-CDS-DEL RV
5′-CCAAATACTCCACACGCAAATGCTGAGGAGGGGCCAGACC-3′
miR-155 BS-UTR-DEL FW
5′-GAGACTGGGTCTCGCTTTGTGATCTTGGCTTACTGCAGCC-3′
miR-155 BS-UTR-DEL RV
5′-GGCTGCAGTAAGCCAAGATCACAAAGCGAGACCCAGTCTC-3′

Drug resistance assays

MTT-based* in vitro *toxicology assay. Five thousand cells treated with different drug concentrations were plated in a 96-well plate (four replicates per condition). After 72 hours, the MTT-based *In Vitro* Toxicology Assay (Sigma-Aldrich) was carried out according to the manufacturer's instructions. Proliferation was analyzed by measuring absorbance at 580 nm with a SpectraMax Plus Micro-Plate Reader (Molecular Devices).

In vitro *cell growth assays.* Twenty-four hours after transfection with anti-miR-155-5p precursor or negative control, A549 cells were treated with 5 μmol/L CDDP for 6h followed by a 24-, 48-, 72-, and 96-hour washout. JM1 stable clones (JM1-LVEV and JM1-LVEV) were treated with 1 μmol/L CDDP for 6 hours followed by a 24, 48, 72, and 96 hours washout, while REH stable clones (REH wt-LVEV, REH wt-155LV, REH shp53-LVEV and REH shp53-155LV) were treated with 0.1 μmol/L doxorubicin for 1 hour followed by a 24-, 48-, 72-, and 96-hour washout. Cells were counted 24, 48, 72, and 96 hours after treatment with the Trypan Blue exclusion assay. Experiments were carried out in triplicates and minimum two independent experiments were performed.

In vitro *proliferation assay.* Twenty-four hours after transfection with hsa-miR-155 inhibitor or negative control, H2009 cells were treated with 10 μmol/L CDDP for 6 hours followed by a 24-, 48-, and 72-hour washout. Cell proliferation was assessed by the CellTiter-Glo Luminescent Cell Viability Assay (Promega) according to the manufacturer's instructions.

Clonogenic assay. A549 cell stably infected with empty lentivirus (A549-LVEV) or with miR-155 overexpressing lentivirus (A549-155LV) were untreated (negative control) or treated with 5 μmol/L CDDP for 6 hours. Twenty-four hours after treatment, cells were trypsinized, and 1,000 cells were plated in triplicates in 60-mm dishes. After 10 days, colonies were fixed with 80% methanol, stained with 0.25% 1,9-dimethyl-methylene blue in 50% ethanol (Sigma-Aldrich), and individual colonies were counted.

***In vivo* orthotopic mouse models**

All mice used in this study were housed and maintained according to guidelines set by the American Association for Accreditation of Laboratory Animal Care and the US Public Health Service policy on Human Care and Use of Laboratory Animals. The mouse study was approved and supervised by The University of Texas MD Anderson Cancer Center Institutional Animal Care and Use Committee, which adheres to the ARRIVE guidelines for *in vivo* experiments. The number of mice was determined based on previous experience with these kind of orthotopic mouse models (31–33), as well as on the power calculations that a group size of 10 would give 80% power to detect changes of 1.686 and 1.638 standard deviations or more in a single group when five, respectively four, groups were considered ($\alpha = 0.05$). Female athymic nude mice between 6 and 8

Published OnlineFirst November 30, 2016; DOI: 10.1158/1078-0432.CCR-16-1025

weeks of age and with a weight of 20–25 g were purchased from the National Cancer Institute, Frederick Cancer Research and Development Center (Frederick, MD).

Orthotopic lung cancer model. Control anti-miR (mirVana miRNA inhibitor negative control #1; Life Technologies) or anti-miR-155 (hsa-miR-155 mirVana miRNA inhibitor; Life Technologies) was incorporated into DOPC nanoliposomes for *in vivo* delivery as previously described (34). The intrapulmonary injections of A549 cells stably infected with either lentivirus containing empty lentiviral vector (A549-LVEV) or with lentivirus containing a miR-155-overexpressing lentiviral vector (A549-155LV) were performed as previously described (32). One week after injection, the mice were randomized in four (initial experiment) or five (second, independent experiment) groups, and treatment with CDDP and/or nanoliposomes (either negative control or miR-155 inhibiting) was started. CDDP (160 μg/mouse) was administered i.p. once a week, while liposomal nanoparticles (200 μg/kg) were administered i.v. twice a week. The treatment schedules can be found in Fig. 2A and Supplementary Fig. S2A. In the initial experiment, out of 40 mice initially injected with A549 cells, two mice died from surgery, and one died from CDDP toxicity 3 weeks after start of treatment. In the second, independent experiment, out of 50 mice initially injected with A549 cells, six died from surgery, and two died from CDDP toxicity 3 to 4 weeks after the start of treatment. After 4, respectively 5, weeks of treatment, the mice were sacrificed and analyzed macroscopically as previously described (32).

MiR-155 expression in tissue sections was analyzed by *in situ* hybridization as previously described (31). Double-digoxigenin (DIG)-labeled locked nucleic acid (LNA) probes for miR-155 (Exiqon) were used.

Cell proliferation, angiogenesis, and microvesicle density and apoptosis were assessed by Ki-67 or CD31 immunostaining, or with the TUNEL assay as previously described (31, 35). Ki-67, CD31, and TUNEL-positive cells were counted in three random fields per slide, and five slides per group were analyzed at 200× magnification.

The expression of TP53 was determined by immunohistochemical analysis using freshly cut frozen mouse tissue. The slides were fixed in cold acetone/acetone + chloroform 1:1/acetone, and blocked with cold-water fish skin gelatin 4% (Electron Microscopy Sciences) in PBS. Slides were incubated overnight at 4°C with primary antibody anti-Tp53 (Cell Signaling Technology), washed with PBS, incubated with the goat anti-rabbit Alexa 594 secondary antibody (The Jackson Laboratory), washed and counterstained with Hoechst. The expression of TP53 was counted in three random fields per slide (one slide per mouse, five slides per group) at 200× magnification.

In vivo toxicology assessment of anti-miR-155

Male CD-1 IGS mice with a weight of 35 to 40 g were purchased from Charles Rivers and randomized into two groups (anti-miR-NC and anti-miR-155; $n = 17$/group). Liposomal control anti-miR-DOPC (anti-miR-NC-DOPC) and anti-miR-155-DOPC nanoparticles were injected into the respective mice i.v. via tail-vein injection at a concentration of 200 μg/kg of body weight. Body weight was measured before and after treatment and was not significantly different between both groups. After 72 hours of treatment, mice were euthanized by exsanguination following IACUC approved protocols. Blood samples and tissues (fixed and embedded in paraffin) were collected at necropsy for further analyses. Blood samples were processed for blood chemistry and hematology. Blood chemistry analyses included blood urea nitrogen content (BUN), aspartate aminotransferase (AST), alanine aminotransferase (ALT), alkaline phosphatase (ALP), and creatinine and lactic dehydrogenase (LDH) and were evaluated on an Integra 400 Plus analyzer (Roche Diagnostics). Hematology analyses consisted of complete blood count [white blood cell (WBC) count, red blood cell (RBC) count, hemoglobin, hematocrit, average volume of RBC (mean corpuscular volume or MCV), average amount of hemoglobin in one RBC (mean corpuscular hemoglobin or MCH), average concentration of hemoglobin in one RBC (MCH concentration or MCHC), red cell distribution width (RDW), platelet and mean platelet volume (MPV)], as well as WBC differential count [levels of segmented neutrophils, lymphocytes, monocytes, eosinophils, basophils and large unstained cells (LUC)], and were evaluated on an Avida 120 Hematology System (Siemens Healthineers). Paraffin-embedded tissue sections were stained with hematoxylin and eosin (H&E) for routine histopathology.

To assess serum cytokine levels, mice were treated with single i.v. injections of either anti-miR-NC-DOPC ($n = 10$) or anti-miR-155-DOPC ($n = 10$). Seventy-two hours after injection, serum was collected using cardiac puncture and analyzed with a Luminex assay (MCYTOMAG-70K-PMX/MULTIPLEX map mouse cytokine/chemokine magnetic bead panel, EMD Millipore) detecting 25 proinflammatory cytokines (G-CSF, GM-CSF, IFNγ, IL1α, IL1β, IL2, IL4, IL5, IL6, IL7, IL9, IL10, IL12 (p40), IL12 (p70), IL13, IL15, IL17, IP10, KC, MCP-1, MIP1α, MIP1β, MIP2, RANTES, and TNFα) using a Luminex 100 system (Luminex), as previously described (36).

Integrated function and pathway analysis

We retrieved experimentally validated miR-155 targets from the following four databases: miRTarBase (http://mirtarbase.mbc.nctu.edu.tw), TarBase (http://diana.imis.athena-innovation.gr/DianaTools/), miRWalk (http://www.umm.uni-heidelberg.de/apps/zmf/mirwalk/), and miRecords (http://c1.accurascience.com/miRecords/). We restricted ourselves to those targets that were supported by strong experimental evidence, such as reporter assay, Western blot, quantitative PCR, and immunoprecipitation. Of the 248 miR-155 targets that were identified, integrated function and pathway analysis was performed using DAVID bioinformatics resources (http://david.abcc.ncifcrf.gov/). We imposed a cutoff of 10% FDR to indicate a statistically significant association between a pathway and the list of mRNA targets of miR-155. The *P* value and false discovery rate were generated by a modified Fisher exact test.

TCGA data analysis

Input data were downloaded from the publicly available data portal of The Cancer Genome Atlas Project (TCGA) at https://gdc.cancer.gov/. Level 3 Illumina RNA-Seq and miRNA-Seq were used for the analysis of mRNA and miRNA expression, respectively. For miRNA-Seq data, we derived the "reads_per_million_miRNA_-mapped" values for mature forms of each microRNA from the "isoform_quantification" files. Patient samples with survival data of 0 "days_to_last_follow_up" were excluded. Data for somatic mutations of *TP53* in TCGA samples were downloaded from the cBio Portal at http://www.cbioportal.org/public-portal/.

Statistical analyses

All patient-related analyses were carried out in the R statistical environment, version 3.0. (http://www.r-project.org/). Survival

Published OnlineFirst November 30, 2016; DOI: 10.1158/1078-0432.CCR-16-1025

analyses were performed as previously described (31) with some modifications. Briefly, for each cohort, a relationship between miR-155/*TP53* expression and overall survival was assessed as follows. Patients were grouped into percentiles according to miR-155 and *TP53* expression. The log-rank test was employed to determine the association between miRNA/mRNA expression and survival. The Kaplan–Meyer method was used to generate survival curves. The *P* value and the cut-off to optimally separate the patients in high and low (min *P* value) miR-155 and *TP53* were recorded. We then considered whether combining inverse expression of miR-155 and *TP53* would associate with survival. We used the following procedure. A fixed cutoff for miR-155 together with a fixed cutoff for *TP53* splits the cohort in four groups corresponding to low or high miR-155 and low or high *TP53* expression. For each pair of cutoffs we contrasted the two groups linked to a negative association: tumors with high levels of miR-155 and low levels of *TP53* versus tumors with low levels of miR-155 and high levels of *TP53*. We recorded the best separation obtained (min *P* value) for the pair and noticed that the difference in median survival time between the two groups contrasted is significantly larger than the difference between the groups classified into high/low based on the expression of miR-155 or *TP53* alone. The relationship between survival and covariates (miR-155 and *TP53* expression levels and available prognostic factors or other clinical parameters) was examined using a Cox proportional hazard model.

For lung adenocarcinoma cases with miR-155 expression, *TP53* mutational status, and survival information available, we checked for a relationship between miR-155 expression, *TP53* expression, and overall survival in patients with wild-type *TP53* and mutated *TP53* in a similar manner as described above. According to the *TP53* mutational status, patients were divided into two groups: (i) those expressing wild-type *TP53* (unmutated) or harboring *TP53* mutations not affecting its protein function (according to the IARC TP53 database p53.iarc.fr), and (ii) those harboring *TP53* mutations that affect TP53 protein function (according to the IARC TP53 database p53.iarc.fr). For each group, Kaplan–Meier overall survival curves were generated for high versus low miR-155, and high miR-155 and low *TP53* versus low miR-155 and high *TP53*.

Statistical analysis of the *in vitro* and *in vivo* data was carried out with GraphPad Prism 6 software. To verify whether data followed a normal distribution, the Shapiro–Wilk normality test was performed, and an unpaired *t* test (normal distribution) or non-parametric Mann–Whitney–Wilcoxon test (nonnormal distribution) was applied to determine *P* values. All tests were two-sided, and *P* values <0.05 were considered statistically significant. Statistical significances are presented according to the following scheme: *, $P < 0.05$; **, $P < 0.01$; ***, $P < 0.001$; ****, $P < 0.0001$.

Results

MiR-155 induces chemoresistance *in vitro*

We treated three different lung cancer and leukemia cell lines with endogenous levels of miR-155 expression and after miR-155 overexpression (either by miR-155 precursor or miR-155 lentivirus) with chemotherapeutic agents commonly used to treat patients: the lung cancer cell line A549 with cisplatin (CDDP, cis-diamminodichloroplatinum) (6, 37), the acute lymphoblastic leukemia (ALL) cell line REH with doxorubicin (38), and the immunoblastic B-cell leukemia/lymphoma cell line JM1 with CDDP (39). As shown in Fig. 1A and B, A549, REH, and JM1 cells overexpresssing miR-155 showed a significantly better viability and displayed significantly lower chemosensitivity when undergoing treatment with CDDP or doxorubicin than cells expressing normal levels of miR-155. In addition, we performed a clonogenic assay for A549 cells stably overexpressing miR-155 (A549-155LV) and treated with CDDP versus control cells (A549-LVEV) treated with CDDP. We observed a significant increase in the number of colonies when miR-155 was overexpressed, further demonstrating the chemoresistance induced by miR-155 (Fig. 1C). Moreover, when we treated the H2009 lung cancer cell line with miR-155 inhibitor and CDDP, we found that these cells grew significantly less than H2009 cells treated with negative control inhibitor and CDDP (Fig. 1D). Of note, when TP53 expression was abolished in REH cells by shRNA treatment, the protective effect to chemotherapeutic agents in cells overexpressing miR-155 disappeared (Fig. 1A, middle; Fig. 1B, middle). Finally, no difference in chemosensitivity was observed after fludarabine treatment and miR-155 overexpression in MEC1 and MEC2 cell lines, both of which carry a deletion of the *TP53* locus (ref. 40; Supplementary Fig. S1). Altogether, these data suggest a role of miR-155 in drug resistance in various types of cancer, including lung cancer and leukemia, for multiple types of chemotherapy.

MiR-155-induced chemoresistance can be reversed *in vivo* by treatment with anti-miR-155-DOPC

To evaluate the *in vivo* involvement of miR-155 in therapy resistance, we established an orthotopic lung cancer mouse model by intrapulmonary injection of A549-LVEV (control) cells or with A549-155LV (miR-155-overexpressing) cells. Two independent experiments were carried out with four (Supplementary Fig. S2) and five (Fig. 2) treatment groups, respectively, in which mice were treated with negative control anti-miR (anti-miR-NC) or with anti-miR-155 alone or in combination with CDDP, according to the schedule in Fig. 2A; Supplementary Fig. S2A. Mice injected with A549-LVEV cells and treated with CDDP and anti-miR-NC showed a decrease in number of tumors, reduced primary tumor size and a reduced aggregate mass of metastases when compared with untreated mice injected with A549-LVEV cells, although this decrease was not significant, indicating that these tumors are sensitive to CDDP, as was expected (Fig. 2B and C; Supplementary Fig. S2B–D). When miR-155 was overexpressed (through injection of A549-155LV cells), the tumors became resistant to CDDP treatment and the administration of anti-miR-155 alone significantly reduced number of tumors, tumor size, and aggregate mass of metastases (Fig. 2B and C). In addition, when anti-miR-155 was combined with CDDP treatment, the chemotherapy resistance was almost completely reversed (Fig. 2B and C; Supplementary Fig. S2B–D). *In situ* hybridization for miR-155 showed an increase of miR-155 expression in miR-155-overexpressing tumors treated with CDDP and anti-miR-NC, and miR-155 levels comparable to or lower than A549-LVEV tumors when miR-155-overexpressing tumors were treated with anti-miR-155 alone or in combination with CDDP (Fig. 2D; Supplementary Fig. S2E). Immunohistochemistry for Ki-67 (proliferation), CD31 (angiogenesis), and the TUNEL (apoptosis) assay suggested that miR-155, even in the presence of CDDP, is able to induce cell proliferation and angiogenesis, and reduce apoptosis, effects that are completely abolished when miR-155 is inhibited (Fig. 2E; Supplementary Fig. S2F). Although treatment

Published OnlineFirst November 30, 2016; DOI: 10.1158/1078-0432.CCR-16-1025

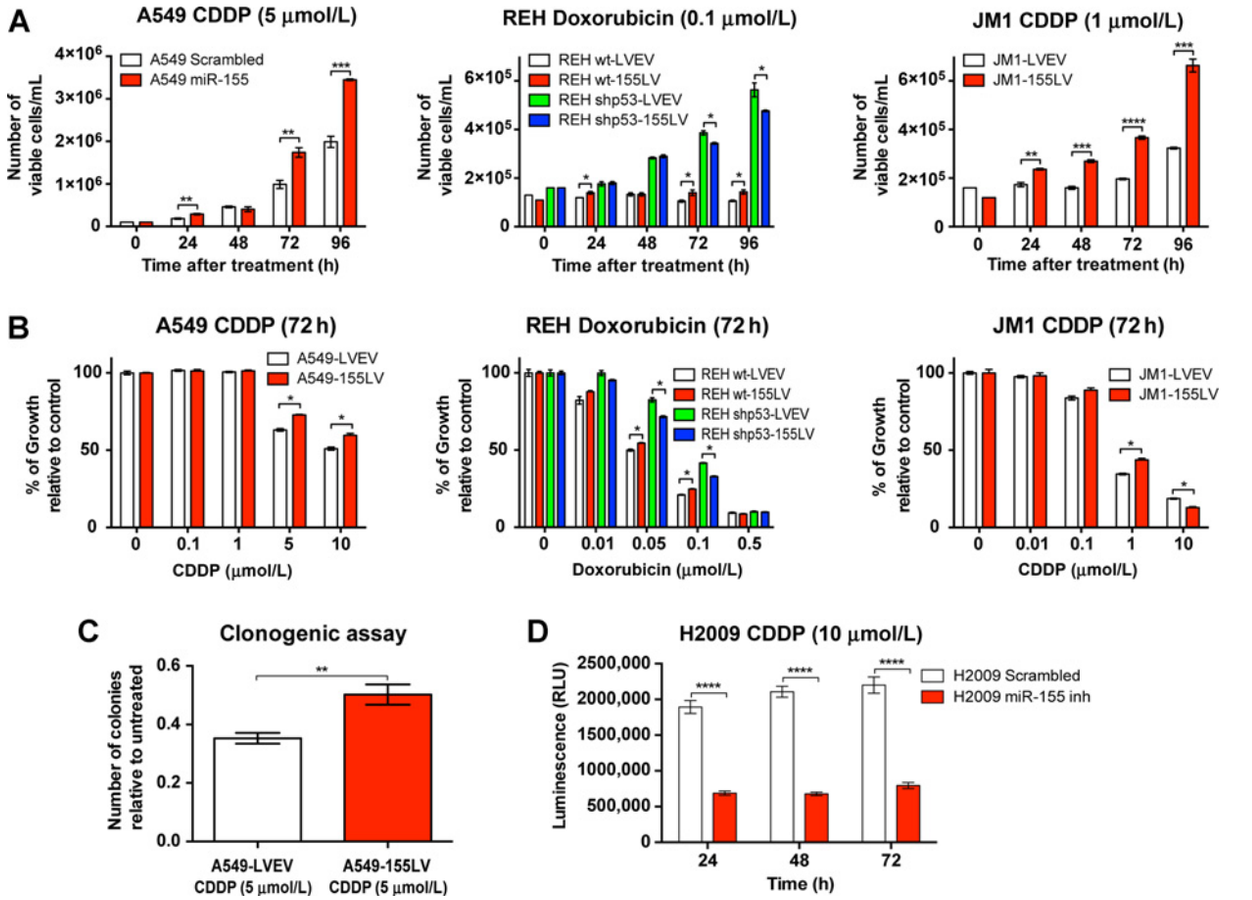

Figure 1.

The effect of miR-155 modulation on drug resistance. **A,** Cell viability and (**B**) dose–response curves for A549 cells treated with CDDP (left graph), REH cells (wt and shp53) treated with doxorubicin (middle) and JM1 cells treated with CDDP (right). **C,** Clonogenic assay of A549 cells treated with CDDP. **D,** Viability assay for H2009 cells treated with CDDP. CDDP, cisplatin; wt, wild-type; shp53, short hairpin for TP53; LVEV, lentivirus empty vector; LV, lentivirus. Error bars, SEM; each assay was performed at least three times.

with anti-miR-155 alone resulted in a significant decrease in proliferation and angiogenesis, and increase in apoptosis, the effects are even more pronounced when anti-miR-155 is combined with CDDP therapy (Fig. 2E). Therefore, the *in vivo* reversion of chemoresistance by anti-miR-155 administration is consistent and reproducible by independent sets of experiments.

Anti-miR-155-DOPC does not induce toxic effects *in vivo*

To assess the *in vivo* toxicity effects of anti-miR-155-DOPC, we evaluated blood chemistry, hematology, cytokine production, and general histology in mice injected with a single dose of either anti-miR-NC-DOPC or anti-miR-155-DOPC (Fig. 3). Blood chemistry analyses for metabolites to assess overall tissue damage (Fig. 3A) and complete hematology investigation of WBC, RBC, and platelets (Fig. 3B and C) showed no significant differences between both groups, except for the platelet count, which was marginally significantly higher in anti-miR-155-DOPC-treated mice ($P = 0.0464$; Fig. 3B). We further performed a cytokine assay detecting 25 proinflammatory cytokines in the serum of mice injected with either anti-miR-NC-DOPC or anti-miR-155-DOPC. With the exception of IL12 (p40), IL17, MIP1α and MIP1β, which showed marginally statistically significant differences, no activation of the immune system was observed (Fig. 3D). Finally, H&E histological analysis showed no inflammatory changes in brain, heart, kidney, liver, lung, and spleen in any of the groups (Fig. 3E). We previously demonstrated that DOPC liposomal nanoparticles are not toxic *in vivo* for doses up to 20 mg/kg for 5 consecutive days (41). These data suggest that the therapeutic effects observed in our *in vivo* orthotopic mouse model are likely caused by targeting of miR-155, rather than by immune induction, and that anti-miR-155-DOPC can be considered non-toxic in mice.

Identification of a miR-155/TP53-negative feedback loop

miR-155 is significantly overexpressed in patients with CLL and deletion of 17p, where the genomic *TP53* locus resides (16), suggesting that TP53 might suppress the expression of miR-155. To assess this hypothesis, we performed ChIP for TP53 in the wild-type ALL cell line REH (REH wt) and showed that TP53 binds to one of three predicted binding sites (BS3) downstream

Published OnlineFirst November 30, 2016; DOI: 10.1158/1078-0432.CCR-16-1025

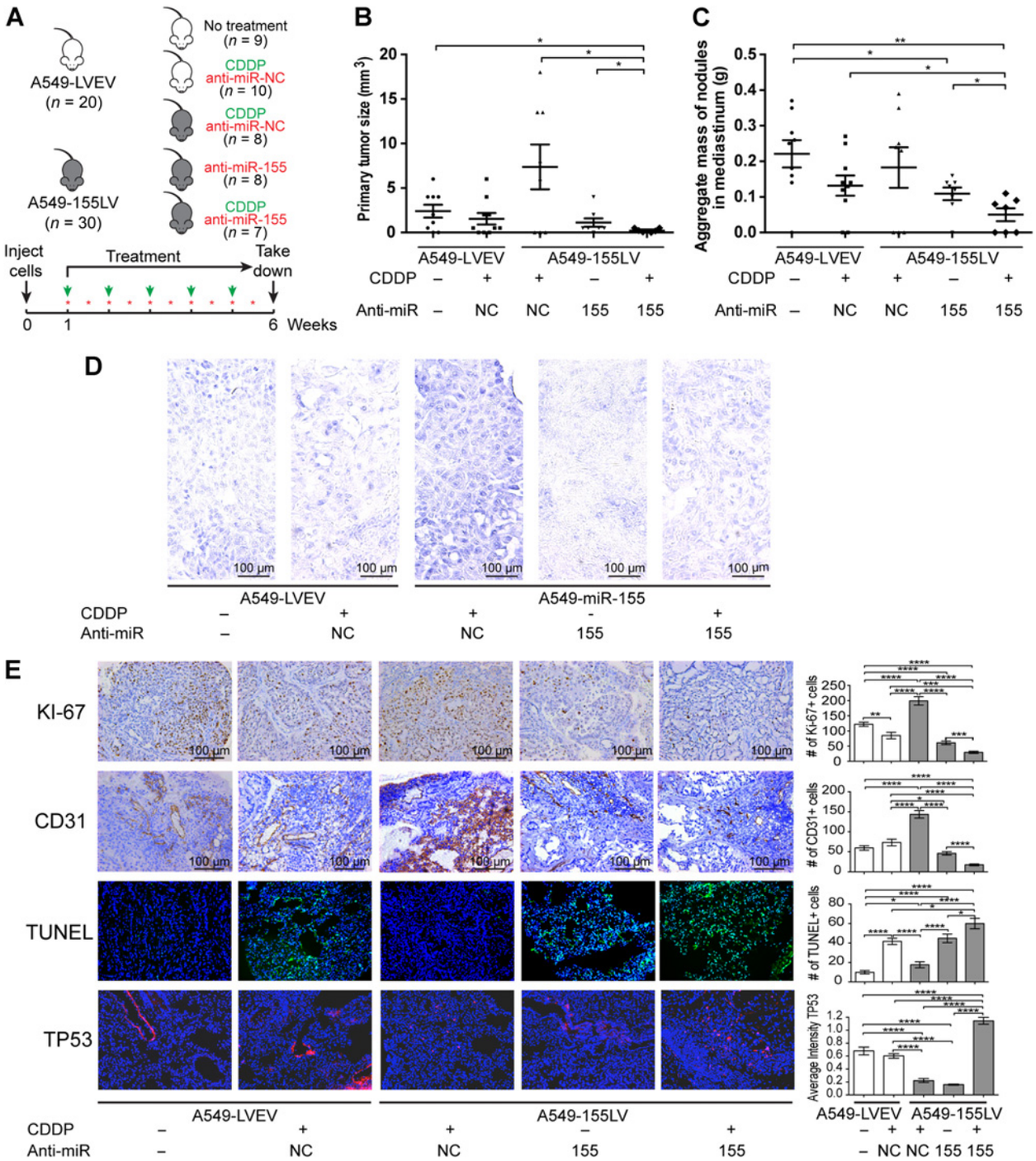

Figure 2.

In vivo orthotopic lung cancer model for the role of miR-155 in chemoresistance. **A,** Injection and treatment schedule for CDDP (green arrows) and anti-miR-negative control (NC) or anti-miR-155 liposomal nanoparticles (red stars) for five different treatment groups: mice that were injected with A549-LVEV cells and untreated (group 1), injected with A549-LVEV cells and treated with anti-miR-NC and CDDP (group 2), injected with A549-155LV cells and treated with anti-miR-NC and CDDP (group 3), injected with A549-155LV cells and treated with anti-miR-155 alone (group 4), and injected with A549-155LV cells and treated with anti-miR-155 and CDDP (group 5). **B** and **C,** Graphs of the primary tumor size (**B**) and the aggregate mass of nodules in the mediastinum (**C**) for each of the five treatment groups. **D,** *In situ* hybridization for miR-155 for each of the five treatment groups. **E,** Immunohistochemical analyses for Ki-67 (proliferation) and CD31 (angiogenesis), as well as the TUNEL assay (apoptosis) and TP53 immunostaining for each of the five treatment groups. Quantifications are presented in the histograms at the right side of the pictures. CDDP, cisplatin; LVEV, lentivirus empty vector; LV, lentivirus; NC, negative control. Error bars, SEM. Scale bars in **D** and **E,** 100 μm. The number of mice in each group is indicated.

Published OnlineFirst November 30, 2016; DOI: 10.1158/1078-0432.CCR-16-1025

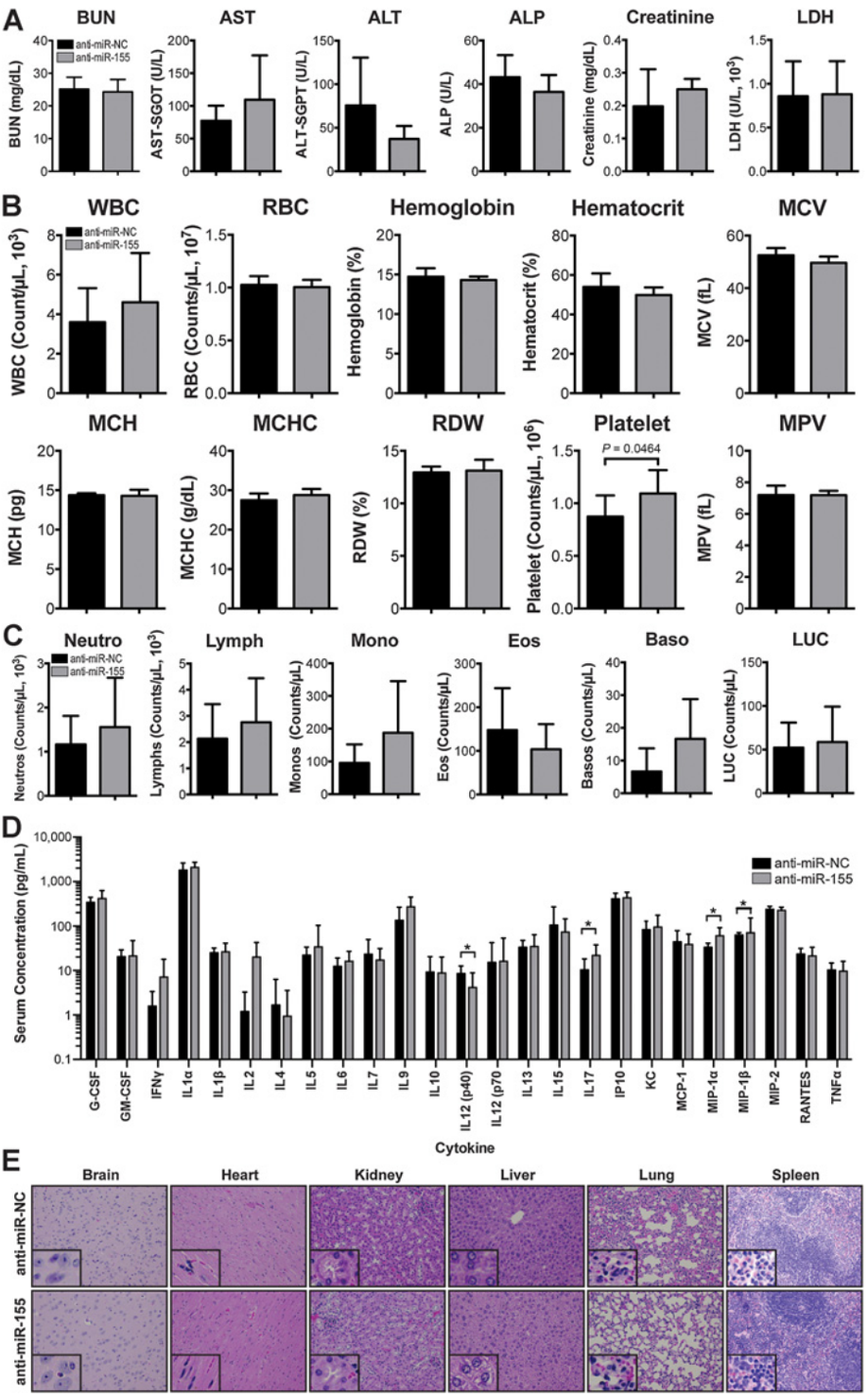

Figure 3.

In vivo toxicology assessment of anti-miR-155-DOPC. **A,** Blood chemistry analyses of BUN, AST, ALT, ALP, creatinine and LDH in mice ($n = 5$/group) treated with anti-miR-NC-DOPC or anti-miR-155-DOPC. **B–C,** Hematology analyses consisting of complete blood count (**B**) including white blood cell (WBC) count, red blood cell (RBC) count, hemoglobin, hematocrit, average volume of RBC (mean corpuscular volume or MCV), average amount of hemoglobin in one RBC (mean corpuscular hemoglobin or MCH), average concentration of hemoglobin in one RBC (MCHC), red cell distribution width (RDW) platelet count and mean platelet volume (MPV), as well as WBC differential count (**C**) including levels of segmented neutrophils, lymphocytes, monocytes, eosinophils, basophils and large unstained cells (LUC) in mice ($n = 10$/group) treated with anti-miR-NC-DOPC or anti-miR-155-DOPC. **D,** Cytokine assay detecting 25 proinflammatory cytokines in the serum of mice ($n = 10$/group) injected with either anti-miR-NC-DOPC or anti-miR-155-DOPC. **E,** H&E staining in brain, heart, kidney, liver, lung, and spleen of mice ($n = 5$/group) treated with anti-miR-NC-DOPC or anti-miR-155-DOPC. Neutro, neutrophils; Lymph, lymphocytes; Mono, monocytes; Eos, eosinophils; Baso, basophils; LUC, large unstained cells. Error bars, SD.

of miR-155 (Fig. 4A and B). A luciferase reporter assay for BS3 confirmed that TP53 inhibits the expression of miR-155 through direct binding in the region downstream of miR-155 (Fig. 4C). The silencing effect was abrogated when BS3 was mutated, further confirming a direct binding of TP53 to BS3 (Fig. 4C). To determine whether miR-155 is involved in a feedback loop, we checked whether overexpression of miR-155 affected TP53 expression. We transfected TP53 wild-type (wt) A549 and H460 cells (42) with miR-155 and observed reduced expression of TP53 protein, as well as of the known miR-155 target TP53INP1 (43, 44) and CDKN1A (p21) (Fig. 4D). When downregulating miR-155 in the H2009 lung cancer cell line harboring a mutation

Published OnlineFirst November 30, 2016; DOI: 10.1158/1078-0432.CCR-16-1025

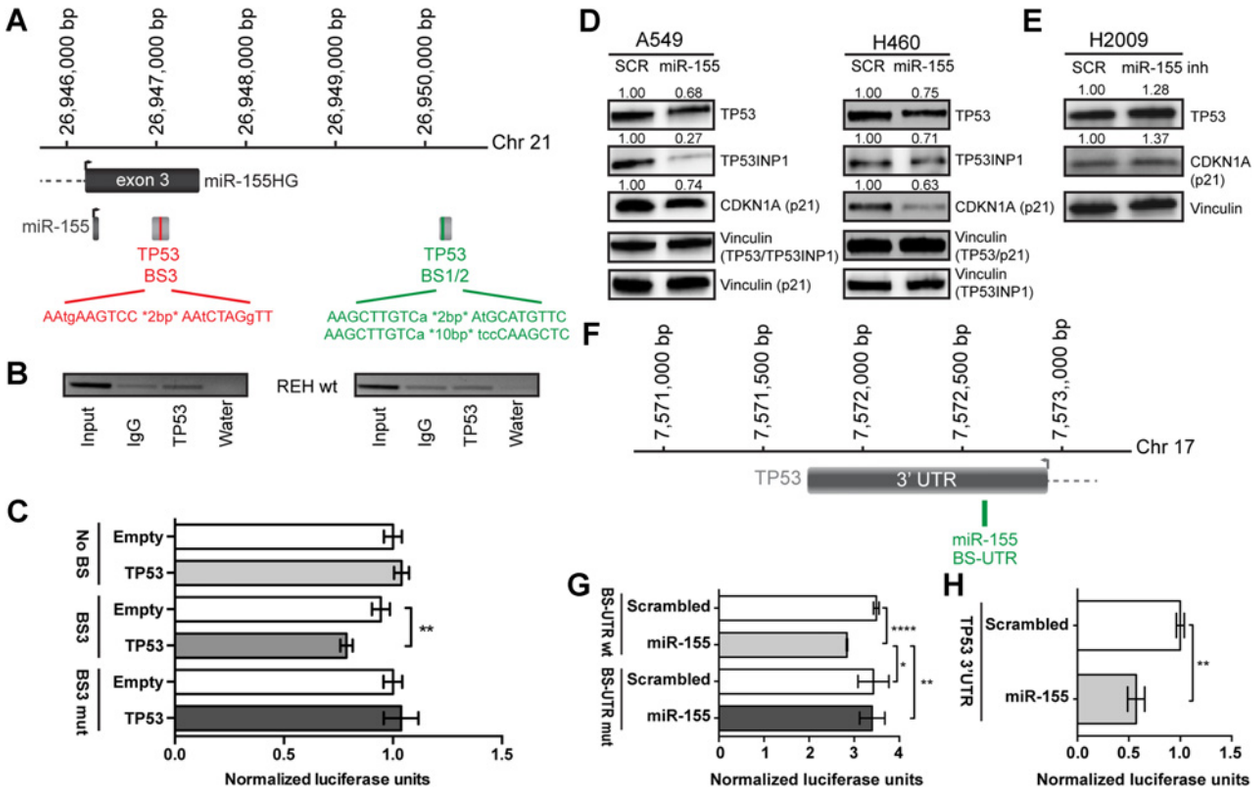

Figure 4.

In vitro validation of a miR-155/TP53-negative feedback loop. **A,** Schematic representation of three predicted TP53 binding sites in the downstream region of miR-155. **B,** ChIP for TP53 binding to BS1/2 and BS3 in REH cells with normal TP53 expression (REH wt). **C,** Luciferase reporter assay and mutagenesis for the TP53 binding site BS3 downstream of miR-155 in A549 cells. **D,** Western blot analysis of A549 and H460 cell lines with baseline miR-155 levels or overexpressing miR-155. **E,** Western blot analysis of H2009 cells with relatively high basal miR-155 expression and after inhibiting miR-155. **F,** Schematic representation of a predicted miR-155 binding site in the 3′ UTR of *TP53* (BS-UTR). **G,** Luciferase reporter assay and mutagenesis for BS-UTR in the TP53-null cell line H1299. **H,** Luciferase reporter assay for the 3′ UTR of *TP53* in the TP53 wild-type cell line H460. BS, binding site; SCR, scrambled. Error bars, SD; each assay was performed at least three times.

in *TP53* that does not affect the miR-155 binding sites, we observed increased TP53 and CDKN1A (p21) protein expression (Fig. 4E). A luciferase reporter assay in the TP53-null cell line H1299 for two identified miR-155 binding sites in the 3′ UTR of *TP53* mRNA (BS-UTR) (Fig. 4F) and in the *TP53* coding sequence (BS-CDS), respectively, showed a direct binding of miR-155 to BS-UTR (Fig. 4G) but not to BS-CDS (data not shown). The silencing effect was abolished when BS-UTR was mutated (Fig. 4G), indicating a direct binding of miR-155 to the 3′ UTR of *TP53*. Similar experiments in the TP53 wild-type cell line H460 showed a reduction in luciferase activity as well (Fig. 4H). Finally, to assess the effects of miR-155 overexpression on TP53 expression *in vivo*, we performed TP53 immunostaining on the mouse tumors and observed a decrease in TP53 expression when miR-155 was overexpressed. Treatment with anti-miR-155 alone did not significantly affect TP53 expression, but a combination of anti-miR-155 with CDDP resulted in a significant increase of TP53 expression (Fig. 2E; Supplementary Fig. S2F). Altogether, these *in vitro* and *in vivo* data demonstrate a negative feedback loop between miR-155 and TP53, which is involved in resistance to chemotherapy.

To understand the biological significance of the newly identified miR-155/TP53 feedback loop, and to determine how our findings fit in with other known functions and targets of miR-155, we performed integrated function and pathway analysis on 248 experimentally validated miR-155 target genes. Thirteen pathways (Supplementary Table S4) were significantly ($P < 0.01$ and FDR < 10%) enriched, the majority of which were related to cancer (pathways in cancer, colorectal cancer, pancreatic cancer), cell growth and death (cell cycle, apoptosis), as well as signal transduction pathways often deregulated in cancer and involved in drug resistance (Wnt signaling pathway, TGFβ signaling pathway, signaling by BMP, signaling by NGF). These pathways closely relate to the roles of miR-155 as an oncogene (45), *TP53* as tumor suppressor and apoptosis inducer (10), and our novel findings of a miR-155/TP53-negative feedback loop involved in resistance to therapy.

High expression of miR-155 and low expression of *TP53* are correlated with survival

MiR-155 was found to have a prognostic impact in patients with various types of cancer (19), including lung cancer (20), leukemia (17, 18), breast cancer (46), renal cell carcinoma (47), glioma (48), colorectal cancer (49), and gallbladder carcinoma (50). We additionally assessed the correlation of miR-155 with survival in two independent and already published CLL cohorts (CLL-NEJM, ref. 23; CLL-Clin Cancer Res, ref. 24), in a new ALL

Published OnlineFirst November 30, 2016; DOI: 10.1158/1078-0432.CCR-16-1025

cohort (ALL-MDACC), and in four lung cancer datasets (two new cohorts, NSCLC-Italy and lung adenocarcinoma-MDACC, and the TCGA cohorts for lung adenocarcinoma and squamous cell carcinoma). To our surprise, we only found a correlation between high expression of miR-155 in the leukemia datasets (Supplementary Fig. S3), but not in any of the lung cancer cohorts (Table 1). We previously showed that a combination of miR-520d-3p and its target EphA2 is a better prognostic factor for ovarian cancer than each gene by itself (31). To investigate whether this is also the case for our newly identified miR-155/TP53-negative feedback loop, we associated miR-155 and *TP53* transcript expression with overall survival (OS) and time-to-progression (TTP) in four sets of lung cancer (Table 1). We used OS as a measure of resistance to therapy. In all cohorts, we found a significant decrease in survival when miR-155 expression was high and *TP53* mRNA expression was low. This was only true for *TP53* mRNA, as no significant associations could be observed in the TCGA lung cancer datasets between miR-155/TP53 protein expression and survival. Unfortunately, no *TP53* expression data were available for any of the CLL and ALL datasets.

When *TP53* mutation status was considered in the lung adenocarcinoma—TCGA subset, only in cases with unmutated (wild-type) *TP53* or with *TP53* mutations not affecting its function, high miR-155 expression (Supplementary Fig. S4A and B), as well as a combination of high miR-155 and low *TP53* expression (Supplementary Fig. S4C and S4D), was significantly associated with shorter OS. Because all tumors in the NSCLC-Italy dataset were selected for having unmutated *TP53*, the same can be concluded for this dataset. Unfortunately, for the lung adenocarcinoma-MDACC and lung squamous cell carcinoma–TCGA datasets, too few patients were left to perform this analysis and get a reliable significance.

Univariate and multivariate analyses containing the miR-155 and *TP53* expression data, several known prognostic factors, and available clinical parameters (Supplementary Table S5), as well as hazard ratio (HR) calculations using the estimated parameters from the Cox models (Supplementary Table S6), confirmed that high miR-155 and low *TP53* mRNA expression or high miR-155 expression (when no *TP53* expression data were available) were independently associated with survival in most datasets (Supplementary Tables S5 and S6). This co-occurrence of high miR-155 expression with low *TP53* mRNA expression appears to be important for predicting survival, as in all analyzed lung cancer datasets, miR-155 expression and *TP53* mRNA expression by itself were not sufficient to be associated with survival. Interestingly, for the leukemia datasets (in which miR-155 expression alone was significantly associated with survival), when considering miR-155 as a continuous variable in the univariate analyses, the significance is lost for all cohorts, except CLL-Clin Cancer Res (Supplementary Table S5). This further supports our concept that a combination of both miR-155 and *TP53* expression represents a better marker to predict survival.

Discussion

Here, we showed for the first time that TP53 and miR-155 are linked in a new feedback mechanism. Besides miR-155, TP53 has been found to be involved in other miRNA regulatory loops, for example, a regulatory feedback loop between TP53 miR-329/300/381/655, and PTTG1 in pituitary tumors (51), a positive feedback loop between miR-192, MDM2, and TP53 in breast cancer (52), and a feed-forward loop involving miR-17/20a, DAPK3, and TP53 (53). In addition, TP53 is regulated through many other mechanisms, of which the most important is MDM2, which blocks the transcriptional activity of TP53 and mediates its ubiquitylation and proteosomal degradation. In turn, TP53 transactivates MDM2 expression to maintain or increase the levels of MDM2 as is appropriate (54). Furthermore, TP53 has two family members, TP63 and TP73, which share significant homology with TP53 and which have several common targets as well as similar tumor suppressive activities as TP53. All three TP53 family members have been found to be involved in chemoresistance (reviewed in refs. 55–57). Moreover, although not yet validated, miR-155 has predicted target sites in *TP63*, *TP73*, and *MDM2* as well (miRWalk2.0). This suggests that the actual involvement of miR-155 in chemoresistance is most likely far more complicated than the simple miR-155/TP53 feedback mechanism we describe here. To which extent MDM2 and the TP53 family members TP63 and TP73 are involved in miR-155-mediated chemoresistance warrants further investigation.

We further demonstrated that the miR-155/TP53 feedback loop is involved in resistance to multiple chemotherapeutic drugs used in treatment combinations in lung cancer (6) and leukemia (38, 58). Through miR-155 downregulation *in vivo*, we successfully resensitized the tumors to chemotherapy and, therefore, this miR-155/TP53 interactor loop could be exploited for miRNA-based therapeutic interventions in cancer patients (59, 60). Others have shown that LNA-based and nanoparticle-based inhibition of miR-155 decreases tumor growth in mouse models of Waldenstrom macroglobulinemia and lymphoma, respectively (61–63). In addition, a recent publication showed that knockdown of miR-155 in the doxorubicin-resistant cell line A549/dox reversed doxorubicin resistance and restored doxorubicin-induced apoptosis and cell-cycle arrest, most likely through downregulation of multidrug resistance genes (*MDR1* and *MRP1*) and the breast cancer resistance protein gene (*BCRP*; ref. 64), further supporting that miR-155 might be a good target in chemosensitization of tumors.

Our *in vivo* toxicology studies did not uncover any adverse effects of anti-miR-155-DOPC in mice. These findings are important, especially in light of the recent early termination of the phase I clinical study of MRX34, the first miRNA-based therapy to be evaluated in clinical trials for the treatment of human cancers, due to multiple immune-related severe adverse events observed in patients receiving MRX34 (ClinicalTrial.gov Identifier NCT01829971). Our approach is to combine chemotherapy with targeted anti-miR-155 therapy, which will significantly reduce the risks of adverse events, since lower doses of both drugs will need to be used to achieve clinical responses. In addition, the used carrier molecule, DOPC liposomal nanoparticles, is currently being tested in a phase I clinical trial (ClinicalTrial.gov Identifier NCT01591356), and so far, no adverse events have been associated with the treatment. This suggests that treatment with anti-miR-155-DOPC will most likely be safe and well tolerated. However, further systematic preclinical safety studies for anti-miR-155-DOPC in large animals are needed before its clinical value can be evaluated.

When we took the *TP53* mutational status into consideration for the survival analysis of the lung adenocarcinoma–TCGA cohort, we observed that miR-155 and the combination of miR-155 and *TP53* are significantly associated with shorter OS, only in cases with unmutated *TP53* or *TP53* mutations not

Published OnlineFirst November 30, 2016; DOI: 10.1158/1078-0432.CCR-16-1025

affecting its function. Similar conclusions could be drawn from the NSCLC-Italy cohort, because all patients were selected for unmutated *TP53* status. In addition, we showed that overexpression of miR-155 in MEC1 and MEC2 cell lines (both carrying a deletion of the *TP53* locus) does not induce chemoresistance to fludarabine treatment (Supplementary Fig. S1), suggesting that there is a difference in response in the context of wild-type and mutant *TP53* alleles. However, as the current data are very limited, further investigation is needed to assess the role of mutant *TP53* versus wild-type *TP53* in the newly identified miR-155/TP53 feedback loop.

In contrast with most of the literature (meta-analyses in refs.19, 20, and 65), we found that in most of the analyzed cancer datasets, miR-155 expression and *TP53* mRNA expression by itself were not sufficient to be associated with OS (Table 1). In fact, significant correlations between miR-155 and survival could only be found in the leukemia cohorts. In addition, a recent meta-analysis evaluating miR-155 as a prognostic factor for survival in 1,557 NSCLC patients from 6 different studies suggested that high expression levels of miR-155 alone may not be significantly related to lung cancer prognosis, except for Asian and American patients (66). Our data further support the importance to consider miRNA (miR-155) and target mRNA (*TP53*) to predict survival. Actually, when combined, we found that high miR-155 and low *TP53* expression significantly correlated with survival in 4 independent lung cancer datasets (Table 1), and that this combination remained independently associated with survival in the datasets analyzed in a multivariate analysis (Supplementary Tables S5 and S6). We recently demonstrated that a combination of miR-520d-3p and its target *EphA2* is a better prognostic factor for ovarian cancer than each gene by itself, and that simultaneous targeting of miRNA/mRNA (miR-520d-3p/*EphA2*) results in a remarkable therapeutic synergy as compared with either monotherapy (31).

In conclusion, our study is innovative due to multiple reasons. We show for the first time that the most frequently altered human tumor suppressor *TP53* is directly targeted by one of the most oncogenic miRNAs, miR-155, and that TP53 directly regulates the expression of this miRNA as a feedback loop. Second, a combination of *TP53* and miR-155 expression seems to be a much better classifier for overall survival of lung cancer and possibly also leukemia, than miR-155 alone. Third, miR-155 and *TP53* and their downstream targets are involved in resistance to multiple types of chemotherapeutic regimens in various hystotypes. Finally, we propose to use anti-miR-155 as an additive to chemotherapy and not as a single agent, as was proposed by others (61–63). This means lower doses of drugs to be used and, consequently, less adverse reactions to occur in clinical trials. The identification of the miR-155/TP53 interaction will favor the advancement of new anti-miR-155-targeted therapies to overcome the development of drug resistance.

Disclosure of Potential Conflicts of Interest

No potential conflicts of interest were disclosed.

Authors' Contributions

Conception and design: K. Van Roosbroeck, T. Setoyama, E. Fuentes-Mattei, R.S. Redis, A. Ferrajoli, G. Lopez-Berestein, M. Fabbri, G.A. Calin

Development of methodology: K. Van Roosbroeck, F. Fanini, T. Setoyama, C. Rodriguez-Aguayo, E. Fuentes-Mattei, I. Vannini, X. Zhang, M. Ferracin, C.V. Pecot, G. Lopez-Berestein, G.A. Calin

Acquisition of data (provided animals, acquired and managed patients, provided facilities, etc.): F. Fanini, C. Rodriguez-Aguayo, E. Fuentes-Mattei, I. Vannini, L. D'Abundo, X. Zhang, M.S. Nicoloso, V. Gonzalez-Villasana, R. Rupaimoole, F. Morabito, A. Neri, V.R. Ruvolo, D. Amadori, L. Abruzzo, S. Calin, A. Ferrajoli, R. Orlowski, M. Negrini, I.I. Wistuba, H.M. Kantarjian, A.K. Sood, G. Lopez-Berestein, M.J. Keating, M. Fabbri

Analysis and interpretation of data (e.g., statistical analysis, biostatistics, computational analysis): K. Van Roosbroeck, F. Fanini, T. Setoyama, C. Ivan, C. Rodriguez-Aguayo, E. Fuentes-Mattei, L. Xiao, R.S. Redis, X. Zhang, V. Gonzalez-Villasana, M. Ferracin, F. Morabito, X. Wang, R. Orlowski, T.M. Lichtenberg, R.V. Davuluri, I. Berindan-Neagoe, M. Negrini, A.K. Sood, G. Lopez-Berestein, M.J. Keating, M. Fabbri, G.A. Calin

Writing, review, and/or revision of the manuscript: K. Van Roosbroeck, F. Fanini, T. Setoyama, E. Fuentes-Mattei, L. Xiao, V. Gonzalez-Villasana, M. Ferracin, F. Morabito, D. Amadori, M.J. You, A. Ferrajoli, R. Orlowski, W. Plunket, M. Negrini, I.I. Wistuba, H.M. Kantarjian, A.K. Sood, G. Lopez-Berestein, M.J. Keating, M. Fabbri, G.A. Calin

Administrative, technical, or material support (i.e., reporting or organizing data, constructing databases): E. Fuentes-Mattei, S. Rossi, P.P. Ruvolo, S. Calin, M.J. Keating

Study supervision: K. Van Roosbroeck, T. Setoyama, A.K. Sood, M. Fabbri, G.A. Calin

Acknowledgments

The authors would like to thank Drs. Evan N. Cohen and James M. Ruben (The University of Texas MD Anderson Cancer Center) for their assistance with the cytokine assay, and A. Gordon Robertson (Canada's Michael Smith Genome Sciences Center) for his assistance with the data collection of the TCGA datasets. We further acknowledge the support of the RNAi and non-coding RNA Center of the University of Texas MD Anderson Cancer Center.

Grant Support

This work was supported in part by a Developmental Research Award by Leukemia SPORE P50 CA100632. Dr. Calin is The Alan M. Gewirtz Leukemia & Lymphoma Society Scholar. This work was supported by National Institutes of Health (NIH/NCATS) grant UH3TR00943-01 through the NIH Common Fund, Office of Strategic Coordination (OSC). Work in Dr. Calin's laboratory is supported in part by the grant NIH/NCI 1 R01 CA182905-01, the UT MD Anderson Cancer Center SPORE in Melanoma grant from NCI (P50 CA093459), Aim at Melanoma Foundation, and the Miriam and Jim Mulva research funds, the UT MD Anderson Cancer Center Brain SPORE (2P50CA127001), a Developmental Research award from Leukemia SPORE, a CLL Moonshot Flagship project, a 2015 Knowledge GAP MDACC grant, an Owens Foundation grant, and the Estate of C.G. Johnson, Jr. Dr. Fabbri is a St. Baldrick Foundation's Scholar and is supported by the Concern Foundation, Hyundai Hope of Wheels, STOP Cancer, Alex's Lemonade, the William Lawrence and Blanche Hughes Foundation, the Jean Perkins Foundation, the Nautica Malibu Triathlon Funds, the award number P30CA014089 from the National Cancer Institute at the National Institutes of Health, the Hugh and Audy Lou Colvin Foundation, and by a Shirley McKernan donation. Dr. Van Roosbroeck was a Henri Benedictus Fellow of the King Baudouin Foundation and the Belgian American Education Foundation. Dr. Berindan-Neagoe was partially financed by a POSCCE grant (709/2010) entitled Clinical and Economical Impact of Proteome and Transcriptome Molecular Profiling in Neoadjuvant Therapy of Triple Negative Breast Cancer (BREASTIMPACT). Drs. Negrini, Neri and Morabito are partially funded by Associazione Italiana per la Ricerca sul Cancro (the Italian Association for Cancer Research (AIRC), "Special Program Molecular Clinical Oncology - 5 per mille" n. 9980, 2010/15). Dr. Fortunato is also supported by the AIRC "Innovative immunotherapeutic treatments of human cancer" n.16695, 2015/18. Part of this work was also supported by National Cancer Institute at the National Institutes of Health (grant number U54 CA151668) and by the Betty Anne Asche Murray Distinguished Professorship (Dr. A.K. Sood).

The costs of publication of this article were defrayed in part by the payment of page charges. This article must therefore be hereby marked *advertisement* in accordance with 18 U.S.C. Section 1734 solely to indicate this fact.

Received April 22, 2016; revised October 19, 2016; accepted November 8, 2016; published OnlineFirst November 30, 2016.

Published OnlineFirst November 30, 2016; DOI: 10.1158/1078-0432.CCR-16-1025

References

1. Berindan-Neagoe I, Monroig Pdel C, Pasculli B, Calin GA. MicroRNAome genome: a treasure for cancer diagnosis and therapy. CA Cancer J Clin 2014;64:311–36.
2. Siegel RL, Miller KD, Jemal A. Cancer statistics, 2015. CA Cancer J Clin 2015;65:5–29.
3. Doroshow JH. Overcoming resistance to targeted anticancer drugs. N Engl J Med 2013;369:1852–3.
4. Calin GA, Croce CM. MicroRNA signatures in human cancers. Nat Rev Cancer 2006;6:857–66.
5. Fabbri M, Calin GA. Epigenetics and miRNAs in human cancer. Adv Genet 2010;70:87–99.
6. Chang A. Chemotherapy, chemoresistance and the changing treatment landscape for NSCLC. Lung Cancer 2011;71:3–10.
7. Panovska A, Smolej L, Lysak D, Brychtova Y, Simkovic M, Motyckova M, et al. The outcome of chronic lymphocytic leukemia patients who relapsed after fludarabine, cyclophosphamide, and rituximab. Eur J Haematol 2013;90:479–85.
8. Dohner H, Stilgenbauer S, Benner A, Leupolt E, Krober A, Bullinger L, et al. Genomic aberrations and survival in chronic lymphocytic leukemia. N Engl J Med 2000;343:1910–6.
9. Van Roosbroeck K, Calin GA. MicroRNAs in chronic lymphocytic leukemia: miRacle or miRage for prognosis and targeted therapies? Sem Oncol 2016;43:209–14.
10. Brosh R, Rotter V. When mutants gain new powers: news from the mutant p53 field. Nat Rev Cancer 2009;9:701–13.
11. Ambros V. MicroRNA pathways in flies and worms: growth, death, fat, stress, and timing. Cell 2003;113:673–6.
12. Volinia S, Calin GA, Liu CG, Ambs S, Cimmino A, Petrocca F, et al. A microRNA expression signature of human solid tumors defines cancer gene targets. Proc Natl Acad Sci U S A 2006;103:2257–61.
13. Eastlack S, Alahari S. MicroRNA and breast cancer: understanding pathogenesis, improving management. Non-Coding RNA 2015;1:17.
14. Kong W, He L, Coppola M, Guo J, Esposito NN, Coppola D, et al. MicroRNA-155 regulates cell survival, growth, and chemosensitivity by targeting FOXO3a in breast cancer. J Biol Chem 2010;285:17869–79.
15. Fabbri M, Bottoni A, Shimizu M, Spizzo R, Nicoloso MS, Rossi S, et al. Association of a microRNA/TP53 feedback circuitry with pathogenesis and outcome of B-cell chronic lymphocytic leukemia. JAMA 2011;305:59–67.
16. Rossi S, Shimizu M, Barbarotto E, Nicoloso MS, Dimitri F, Sampath D, et al. microRNA fingerprinting of CLL patients with chromosome 17p deletion identify a miR-21 score that stratifies early survival. Blood 2010;116:945–52.
17. Ferrajoli A, Shanafelt TD, Ivan C, Shimizu M, Rabe KG, Nouraee N, et al. Prognostic value of miR-155 in individuals with monoclonal B-cell lymphocytosis and patients with B chronic lymphocytic leukemia. Blood 2013;122:1891–9.
18. Marcucci G, Maharry KS, Metzeler KH, Volinia S, Wu YZ, Mrozek K, et al. Clinical role of microRNAs in cytogenetically normal acute myeloid leukemia: miR-155 upregulation independently identifies high-risk patients. J Clin Oncol 2013;31:2086–93.
19. He J, Zhang F, Wu Y, Zhang W, Zhu X, He X, et al. Prognostic role of microRNA-155 in various carcinomas: results from a meta-analysis. Dis Markers 2013;34:379–86.
20. Xu TP, Zhu CH, Zhang J, Xia R, Wu FL, Han L, et al. MicroRNA-155 expression has prognostic value in patients with non-small cell lung cancer and digestive system carcinomas. Asian Pac J Cancer Prev 2013;14:7085–90.
21. Kim JH, Kim WS, Park C. Epstein-Barr virus latent membrane protein-1 protects B-cell lymphoma from rituximab-induced apoptosis through miR-155-mediated Akt activation and up-regulation of Mcl-1. Leuk Lymphoma 2012;53:1586–91.
22. Pu J, Bai D, Yang X, Lu X, Xu L, Lu J. Adrenaline promotes cell proliferation and increases chemoresistance in colon cancer HT29 cells through induction of miR-155. Biochem Biophys Res Commun 2012;428:210–5.
23. Calin GA, Ferracin M, Cimmino A, Di Leva G, Shimizu M, Wojcik SE, et al. A MicroRNA signature associated with prognosis and progression in chronic lymphocytic leukemia. N Engl J Med 2005;353:1793–801.
24. Negrini M, Cutrona G, Bassi C, Fabris S, Zagatti B, Colombo M, et al. microRNAome expression in chronic lymphocytic leukemia: comparison with normal B-cell subsets and correlations with prognostic and clinical parameters. Clin Cancer Res 2014;20:4141–53.
25. Ruvolo VR, Kurinna SM, Karanjeet KB, Schuster TF, Martelli AM, McCubrey JA, et al. PKR regulates B56(alpha)-mediated BCL2 phosphatase activity in acute lymphoblastic leukemia-derived REH cells. J Biol Chem 2008;283:35474–85.
26. Challagundla KB, Wise PM, Neviani P, Chava H, Murtadha M, Xu T, et al. Exosome-mediated transfer of microRNAs within the tumor microenvironment and neuroblastoma resistance to chemotherapy. J Natl Cancer Inst 2015;107; pii: djv135. doi: 10.1093/jnci/djv135. Print 2015 Jul.
27. Ling H, Pickard K, Ivan C, Isella C, Ikuo M, Mitter R, et al. The clinical and biological significance of MIR-224 expression in colorectal cancer metastasis. Gut 2016;65:977–89.
28. de Stanchina E, Querido E, Narita M, Davuluri RV, Pandolfi PP, Ferbeyre G, et al. PML is a direct p53 target that modulates p53 effector functions. Mol Cell 2004;13:523–35.
29. Yoon H, Liyanarachchi S, Wright FA, Davuluri R, Lockman JC, de la Chapelle A, et al. Gene expression profiling of isogenic cells with different TP53 gene dosage reveals numerous genes that are affected by TP53 dosage and identifies CSPG2 as a direct target of p53. Proc Natl Acad Sci U S A 2002;99:15632–7.
30. Rehmsmeier M, Steffen P, Hochsmann M, Giegerich R. Fast and effective prediction of microRNA/target duplexes. Rna 2004;10:1507–17.
31. Nishimura M, Jung EJ, Shah MY, Lu C, Spizzo R, Shimizu M, et al. Therapeutic synergy between microRNA and siRNA in ovarian cancer treatment. Cancer Discov 2013;3:1302–15.
32. Pecot CV, Rupaimoole R, Yang D, Akbani R, Ivan C, Lu C, et al. Tumour angiogenesis regulation by the miR-200 family. Nat Commun 2013;4:2427.
33. Pecot CV, Wu SY, Bellister S, Filant J, Rupaimoole R, Hisamatsu T, et al. Therapeutic silencing of KRAS using systemically delivered siRNAs. Mol Cancer Ther 2014;13:2876–85.
34. Yang D, Sun Y, Hu L, Zheng H, Ji P, Pecot CV, et al. Integrated analyses identify a master microRNA regulatory network for the mesenchymal subtype in serous ovarian cancer. Cancer Cell 2013;23:186–99.
35. Shahzad MM, Mangala LS, Han HD, Lu C, Bottsford-Miller J, Nishimura M, et al. Targeted delivery of small interfering RNA using reconstituted high-density lipoprotein nanoparticles. Neoplasia 2011;13:309–19.
36. Aslan B, Monroig P, Hsu MC, Pena GA, Rodriguez-Aguayo C, Gonzalez-Villasana V, et al. The ZNF304-integrin axis protects against anoikis in cancer. Nat Commun 2015;6:7351.
37. Kelland L. The resurgence of platinum-based cancer chemotherapy. Nat Rev Cancer 2007;7:573–84.
38. Garcia-Manero G, Kantarjian HM. The hyper-CVAD regimen in adult acute lymphocytic leukemia. Hematol Oncol Clin North Am 2000;14:1381–96, x-xi.
39. Hou Y, Wang HQ, Ba Y. Rituximab, gemcitabine, cisplatin, and dexamethasone in patients with refractory or relapsed aggressive B-cell lymphoma. Med Oncol 2012;29:2409–16.
40. Stacchini A, Aragno M, Vallario A, Alfarano A, Circosta P, Gottardi D, et al. MEC1 and MEC2: two new cell lines derived from B-chronic lymphocytic leukaemia in prolymphocytoid transformation. Leuk Res 1999;23:127–36.
41. Shen H, Rodriguez-Aguayo C, Xu R, Gonzalez-Villasana V, Mai J, Huang Y, et al. Enhancing chemotherapy response with sustained EphA2 silencing using multistage vector delivery. Clin Cancer Res 2013;19:1806–15.
42. O'Connor PM, Jackman J, Bae I, Myers TG, Fan S, Mutoh M, et al. Characterization of the p53 tumor suppressor pathway in cell lines of the National Cancer Institute anticancer drug screen and correlations with the growth-inhibitory potency of 123 anticancer agents. Cancer Res 1997;57:4285–300.
43. Gironella M, Seux M, Xie MJ, Cano C, Tomasini R, Gommeaux J, et al. Tumor protein 53-induced nuclear protein 1 expression is repressed by miR-155, and its restoration inhibits pancreatic tumor development. Proc Natl Acad Sci U S A 2007;104:16170–5.
44. Zhang CM, Zhao J, Deng HY. MiR-155 promotes proliferation of human breast cancer MCF-7 cells through targeting tumor protein 53-induced nuclear protein 1. J Biomed Sci 2013;20:79.
45. Faraoni I, Antonetti FR, Cardone J, Bonmassar E. miR-155 gene: a typical multifunctional microRNA. Biochim Biophys Acta 2009;1792:497–505.

46. Chen J, Wang BC, Tang JH. Clinical significance of microRNA-155 expression in human breast cancer. J Surg Oncol 2012;106:260–6.
47. Shinmei S, Sakamoto N, Goto K, Sentani K, Anami K, Hayashi T, et al. MicroRNA-155 is a predictive marker for survival in patients with clear cell renal cell carcinoma. Int J Urol 2013;20:468–77.
48. Sun J, Shi H, Lai N, Liao K, Zhang S, Lu X. Overexpression of microRNA-155 predicts poor prognosis in glioma patients. Med Oncol 2014;31:911.
49. Shibuya H, Iinuma H, Shimada R, Horiuchi A, Watanabe T. Clinicopathological and prognostic value of microRNA-21 and microRNA-155 in colorectal cancer. Oncology 2010;79:313–20.
50. Zhang XL, Chen JH, Qin CK. MicroRNA-155 expression as a prognostic factor in patients with gallbladder carcinoma after surgical resection. Int J Clin Exp Med 2015;8:21241–6.
51. Liang HQ, Wang RJ, Diao CF, Li JW, Su JL, Zhang S. The PTTG1-targeting miRNAs miR-329, miR-300, miR-381, and miR-655 inhibit pituitary tumor cell tumorigenesis and are involved in a p53/PTTG1 regulation feedback loop. Oncotarget 2015;6:29413–27.
52. Moore R, Ooi HK, Kang T, Bleris L, Ma L. MiR-192-Mediated positive feedback loop controls the robustness of stress-induced p53 oscillations in breast cancer cells. PLoS Comput Biol 2015;11:e1004653.
53. Cai Z, Cao R, Zhang K, Xue Y, Zhang C, Zhou Y, et al. Oncogenic miR-17/20a forms a positive feed-forward loop with the p53 Kinase DAPK3 to promote tumorigenesis. J Biol Chem 2015;290:19967–75.
54. Meek DW. Regulation of the p53 response and its relationship to cancer. Biochem J 2015;469:325–46.
55. Ferraiuolo M, Di Agostino S, Blandino G, Strano S. Oncogenic Intra-p53 family member interactions in human cancers. Front Oncol 2016;6:77.
56. Pflaum J, Schlosser S, Muller M. p53 Family and cellular stress responses in cancer. Front Oncol 2014;4:285.
57. Venkatanarayan A, Raulji P, Norton W, Flores ER. Novel therapeutic interventions for p53-altered tumors through manipulation of its family members, p63 and p73. Cell Cycle 2016;15:164–71.
58. Calin GA, Croce CM. Genomics of chronic lymphocytic leukemia microRNAs as new players with clinical significance. Sem Oncol 2006;33:167–73.
59. Ling H, Fabbri M, Calin GA. MicroRNAs and other non-coding RNAs as targets for anticancer drug development. Nat Rev Drug Discov 2013;12:847–65.
60. Berindan-Neagoe I, Calin GA. Molecular pathways: microRNAs, cancer cells, and microenvironment. Clin Cancer Res 2014;20:6247–53.
61. Babar IA, Cheng CJ, Booth CJ, Liang X, Weidhaas JB, Saltzman WM, et al. Nanoparticle-based therapy in an in vivo microRNA-155 (miR-155)-dependent mouse model of lymphoma. Proc Natl Acad Sci U S A 2012;109:E1695–704.
62. Zhang Y, Roccaro AM, Rombaoa C, Flores L, Obad S, Fernandes SM, et al. LNA-mediated anti-miR-155 silencing in low-grade B-cell lymphomas. Blood 2012;120:1678–86.
63. Cheng CJ, Bahal R, Babar IA, Pincus Z, Barrera F, Liu C, et al. MicroRNA silencing for cancer therapy targeted to the tumour microenvironment. Nature 2015;518:107–10.
64. Lv L, An X, Li H, Ma L. Effect of miR-155 knockdown on the reversal of doxorubicin resistance in human lung cancer A549/dox cells. Oncol Lett 2016;11:1161–6.
65. Wang Y, Li J, Tong L, Zhang J, Zhai A, Xu K, et al. The prognostic value of miR-21 and miR-155 in non–small-cell lung cancer: a meta-analysis. Jpn J Clin Oncol 2013;43:813–20.
66. Wang F, Zhou J, Zhang Y, Wang Y, Cheng L, Bai Y, et al. The value of MicroRNA-155 as a prognostic factor for survival in non-small cell lung cancer: a meta-analysis. PloS One 2015;10:e0136889.

Published OnlineFirst November 30, 2016; DOI: 10.1158/1078-0432.CCR-16-1025

Clinical Cancer Research

Combining Anti-Mir-155 with Chemotherapy for the Treatment of Lung Cancers

Katrien Van Roosbroeck, Francesca Fanini, Tetsuro Setoyama, et al.

Clin Cancer Res 2017;23:2891-2904. Published OnlineFirst November 30, 2016.